

## Damage imaging in a laminated composite plate using an air-coupled time reversal mirror

P.-Y. Le Bas,<sup>1,a)</sup> M. C. Remillieux,<sup>1,a),b)</sup> L. Pieczonka,<sup>2,c)</sup> J. A. Ten Cate,<sup>1</sup> B. E. Anderson,<sup>1</sup> and T. J. Ulrich<sup>1</sup>

<sup>1</sup>Geophysics Group (EES-17), Los Alamos National Laboratory, Los Alamos, New Mexico 87545, USA

<sup>2</sup>Department of Robotics and Mechatronics, AGH University of Science and Technology, 30-059 Krakow, Poland

(Received 2 September 2015; accepted 23 October 2015; published online 3 November 2015)

We demonstrate the possibility of selectively imaging the features of a barely visible impact damage in a laminated composite plate by using an air-coupled time reversal mirror. The mirror consists of a number of piezoelectric transducers affixed to wedges of power law profiles, which act as unconventional matching layers. The transducers are enclosed in a hollow reverberant cavity with an opening to allow progressive emission of the ultrasonic wave field towards the composite plate. The principle of time reversal is used to focus elastic waves at each point of a scanning grid spanning the surface of the plate, thus allowing localized inspection at each of these points. The proposed device and signal processing removes the need to be in direct contact with the plate and reveals the same features as vibrothermography and more features than a C-scan. More importantly, this device can decouple the features of the defect according to their orientation, by selectively focusing vector components of motion into the object, through air. For instance, a delamination can be imaged in one experiment using out-of-plane focusing, whereas a crack can be imaged in a separate experiment using in-plane focusing. This capability, inherited from the principle of time reversal, cannot be found in conventional air-coupled transducers. © 2015 AIP Publishing LLC. [<http://dx.doi.org/10.1063/1.4935210>]

Imaging selective features of a complex scatterer buried in an object, according to the physical properties and orientations of these features, has a number of practical applications in biomedical engineering, geophysics, and nondestructive testing (NDT). The ability of doing so without contact offers the possibility of rapidly scanning large areas and inspecting delicate structures, thus reducing the test time by orders of magnitude. In the field of NDT, where ultrasound-based techniques remain the most commonly used, imaging through air (without contact) has been limited by the large impedance mismatch between the source transducers and the air, and between the air and the object to be imaged. The transfer of energy from the source transducer to the object can be enhanced by minimizing the impedance contrast between the transducer and air, by acoustic focusing, and combination thereof.<sup>1,2</sup> Acoustic focusing can be achieved by shape optimization, e.g., a transducer with a parabolic shape<sup>3</sup> or a single source embedded in an ellipsoidal reflector.<sup>4</sup> However, the focal point of these devices is usually fixed and cannot be moved without moving the device itself. Acoustic focusing can also be achieved with signal processing techniques including phased arrays<sup>5</sup> (i.e., parabolic delays between the elements of a linear array of transducers) and time reversal mirrors<sup>6</sup> (TRM). Unlike phased-arrays, the TRM are robust to the heterogeneity of the medium and do

not need *a priori* knowledge of the time delays between the transducers and the focal point, as demonstrated multiple times for the NDT applications.<sup>7-9</sup> In a bounded medium, the quality of the spatio-temporal focusing is mainly controlled by the number of transducers used in the TRM, the duration of the recorded signal, the modal density of the medium, and the amount of damping. If the modal density is sufficiently large and damping is sufficiently small, the TRM can be reduced to a single element. This is possible because the multiple reflections of the waves onto the boundaries of the medium act as virtual sources. This idea has led directly to the development of chaotic cavity transducers, which consist of one piezoelectric transducer affixed to a solid piece of material with an arbitrary shape, for the generation of elastic waves in solids with contact.<sup>10-12</sup> Such device will enhance scattering, break any symmetry that could potentially exist in the system, and considerably reduce the complexity of the experimental apparatus. The cavity can also include multiple elements to increase the amplitude of the focused energy. The concept of chaotic cavity has also been applied to air-coupled transduction.<sup>13-15</sup> The device proposed by Le Bas *et al.*<sup>14</sup> could focus acoustic waves onto the surface of an object. However, preliminary experiments (unpublished) revealed that it could not be used, at that time, for damage imaging, because of the insufficient amount of the energy transmitted to the object. In this letter, we demonstrate the feasibility of using a TRM for exhaustive and selective damage imaging in a plate.

The test sample was a laminated composite plate with in-plane dimensions of 150 × 300 mm and a thickness of 2 mm. The plate was manufactured from carbon/epoxy (Seal

<sup>a)</sup>P.-Y. Le Bas and M. C. Remillieux contributed equally to this work.

<sup>b)</sup>Author to whom correspondence should be addressed. Electronic mail: mcr1@lanl.gov.

<sup>c)</sup>This research was performed while L. Pieczonka was a visiting scientist in the Geophysics Group at Los Alamos National Laboratory, Los Alamos, New Mexico 87545, USA.

HS160/REM) unidirectional prepreg plies. The stacking sequence of the laminate was  $[0_3/90_3]_s$ . A barely visible impact damage (BVID) was introduced into the plate from a low velocity impact test. In this test, the plate was simply supported on the rectangular opening of a rigid post while a drop-weight testing machine was used to impact the plate at the center of the opening. The energy of the impact on the plate was 2.1 J, which was evaluated by measuring the velocities of the impactor immediately before and after the impact. The BVID was first imaged with vibrothermography and ultrasonic C-scan. The results obtained with these traditional techniques will be used as references to validate the device described in this letter.

In vibrothermography, external energy is delivered to the structure by contact ultrasonic vibration, while an infrared camera is used to record the temperature distribution on the surface of the sample.<sup>16,17</sup> This technique relies on the fact that a defect (e.g., delamination and crack) dissipates more energy in the form of heat, mainly due to the mechanism of friction, than the intact portion of the sample. In the present study, the Monit SHM vibrothermographic test system using the 35 kHz ultrasonic excitation column was used. FLIR Silver 420M photon detector camera was used to acquire thermal image sequences. The ultrasonic transducer excited the plate for 500 ms. The thermographic camera acquired the signal at a frame rate of 100 Hz for 3 s. The image of the BVID obtained with vibrothermography is shown in Fig. 1(a). It reveals two distinct features, namely, two delaminations centered around the impact point and a crack going through the delaminations. For the ultrasonic C-scan, the composite plate was immersed in water and scanned at normal incidence in pulse-echo mode by using a focused broadband transducer with a diameter of 3.2 mm, a focal length of 18 mm, and a center frequency of 22 MHz. If the probe is used on the intact portion of the plate, at least

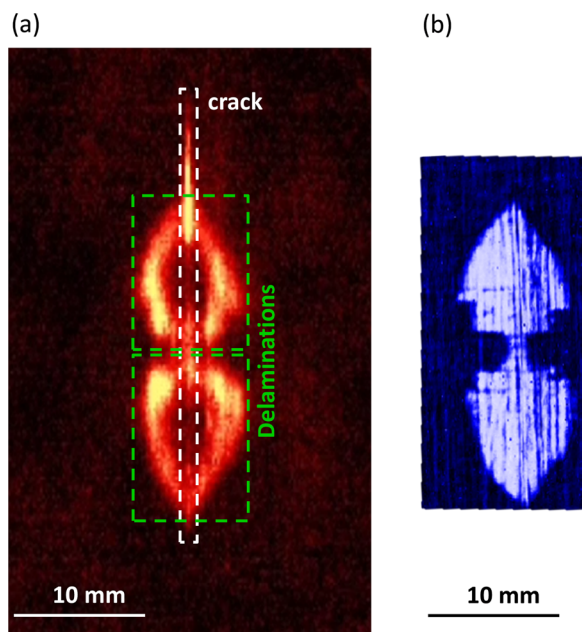


FIG. 1. Images of the BVID obtained with (a) vibrothermography and (b) ultrasonic C-scan.

two echoes will be generated in the measured signal due to the reflections of the ultrasonic waves on the front and back surfaces. Additional echoes will be generated in between the main echoes when a delamination is present.<sup>18</sup> The image obtained from a C-scan performed around the BVID with a resolution of 0.2 mm is shown in Fig. 1(b). The C-scan provides a very sharp image of the delamination but cannot detect the presence of a crack, which is perpendicular to the surface of the plate.

We designed and fabricated an air-coupled TRM, the operating principle of which is depicted in Fig. 2(a), to achieve a spatio-temporal focus of elastic wave energy onto the surface of a plate. The elastic response at the focal point is then used for detecting the presence of a defect. The TRM is essentially a multi-element, air-coupled chaotic cavity. It consists of a hollow reverberant cavity enclosing a number of piezoelectric transducers. The cavity creates a scattered ultrasonic wave field inside and contains an opening to allow a progressive emission of the wave field towards the plate. The piezoelectric transducers are affixed to wedges of cubic profile, which act as unconventional matching layers by providing high amplitude and broadband ultrasonic radiation to the surrounding air.<sup>19,20</sup> The design of these wedges is based on the acoustic black hole effect. Theoretically, a flexural wave slows down and eventually stops when traveling down a wedge with a thickness decreasing smoothly to zero according to a power law.<sup>21,22</sup> Practically, this means that elastic waves become trapped in the thinnest portion of the wedge, where the impedance match with air is the best. This

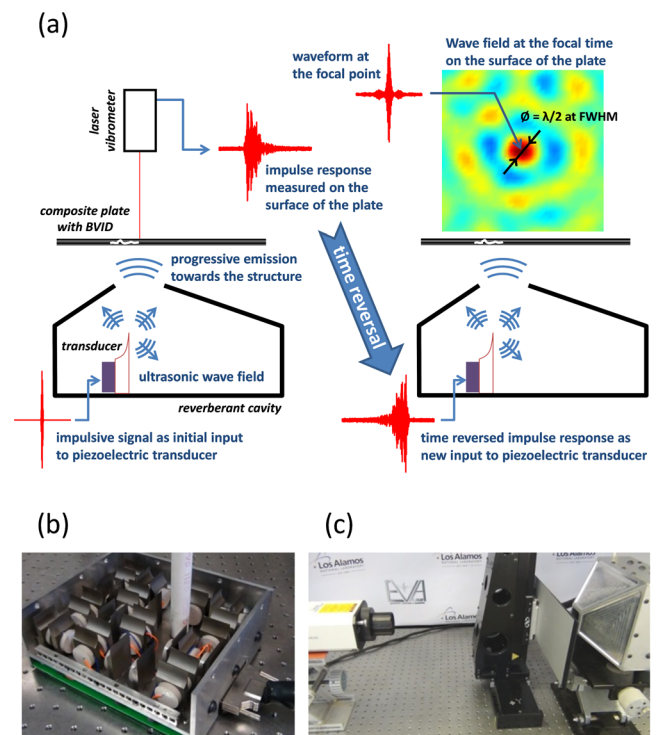


FIG. 2. (a) Operating principle of the air-coupled TRM used to achieve spatio-temporal focus of elastic wave energy onto the surface of a plate; (b) prototype of the TRM showing 32 independently controlled piezoelectric transducers affixed to wedges of cubic profile; and (c) experimental setup to image BVID in the laminated composite plate using the TRM as a source and an out-of-plane laser vibrometer as a receiver. In (a), FWHM indicates that the size of the focal spot is measured at full width half maximum.

hardware is operated as a TRM, which is a two-step process. In the first step, an impulsive voltage signal is applied to the piezoelectric element. This element and the wedge radiate ultrasonic waves into the reverberant cavity, up to the surface of the plate. Meanwhile, a laser vibrometer records the velocity field onto the surface of the plate. The recorded signal is a complex impulse response due to the scattering of elastic waves inside the wedge, ultrasonic waves inside the reverberant cavity, and elastic waves inside the composite plate. In the second step, the impulse response recorded by the laser is time reversed, normalized in amplitude, and applied as a voltage signal to the piezoelectric element. As a result of reciprocity in space and time-reversal invariance of the wave equation, the elastic wave energy focuses in space and time onto the surface of the plate, where the impulse response was originally recorded by the laser vibrometer. The spatial extent of the focal spot measured at full width half maximum (FWHM) is theoretically, according to the diffracting limit, equal to a half wavelength at the center frequency of the reconstructed pulse. However, there are imperfections in this reconstruction process, mainly because the directional information of the energy received in the first step is typically not used, attenuation that exists in a realistic system, and because a limited (as opposed to infinite) acquisition time of the forward propagation signal is available. In practice, this results in side lobes both in space and time, as shown in Fig. 2(a). For simplicity, the TR process was described with only one transducer, whereas the actual prototype shown in Fig. 2(b) is made of 32 independently controlled transducers. In the experiments reported in this letter, only 16 active elements were used. Note that, in the case of a multi-element TRM, the first step of the TR process is repeated for each element. In the second step, all transducers are driven simultaneously, with the individual signals acquired during the first step.

The experimental setup consisting of the laminated composite plate, the TRM, and an out-of-plane laser vibrometer (Polytec OFV-303) is shown in Fig. 2(c). The stand-off distance between the plate and the opening of the TRM was 2 cm. In this experiment, we focused the out-of-plane component of the particle velocity on the surface of the plate because of the particular choice of the receiver. In another experiment, we also focused the in-plane component of the particle velocity, using the same TRM and an in-plane laser vibrometer (Polytec OFV-552). The possibility of selectively focusing (individually or collectively) vector components of motion on the surface of a solid by using a scalar source, a 3D receiver (or at least a receiver capable of sensing more than one motion component), and the principle of TR was demonstrated by Ulrich *et al.*<sup>23</sup> This idea is exploited in this letter for focusing on different vector components of motion and imaging selective features of the damage. This capability of the TRM cannot be achieved by conventional air-coupled transducers.

We defined a scanning grid spanning an area of  $40 \times 20 \text{ mm}^2$  with a resolution of 0.5 mm (a total of 3321 points) around the BVID. In principle, the two steps of the TR process should be repeated for each point of the scanning grid. Here, the first step of the TR process was conducted only once for all transducers, using the first point of the

scanning grid. In this first step, the signal applied to the transducers is a 5-cycle toneburst centered at 100 kHz in a Hanning window, with a peak amplitude of 200 V after amplification. The signals are generated using NI-7852R arbitrary waveform generator and amplified via amplifiers 9400 from Tabor electronics. The impulse responses acquired during this step were used to focus elastic wave energy at all the other points of the grid. Such strategy resulted in reducing the test time by orders of magnitude without compromising on the quality of the TR focus and imaging process. This is possible assuming that all the major reflections contributing to the time reversal process occur inside the cavity. A comparison (not shown) between this experiment and a similar one, where the first step of time reversal is repeated at each scan point, shows little to no difference in the result obtained, validating that assumption. Once focusing has been achieved and recorded at all grid points, the post-processing steps, described in Fig. 3, can be applied. The signals acquired on the scanning grid are compared, in the frequency domain, to a reference signal acquired at the first point of the scanning grid, which is assumed to be located in an intact region of the sample. Imaging is possible because signals measured on the BVID differ in terms of amplitude and frequency content from the signal measured at the reference point. The difference between the magnitudes of the spectra measured away from and at the reference point is integrated in frequency, from  $f_{min} = 90 \text{ kHz}$  to  $f_{max} = 110 \text{ kHz}$ , i.e., around the center frequency of the toneburst. Differences between the measured spectra are also observed at lower frequencies, around 75 kHz, which is the resonance frequency of the piezoelectric transducers. Using higher frequencies for the integration

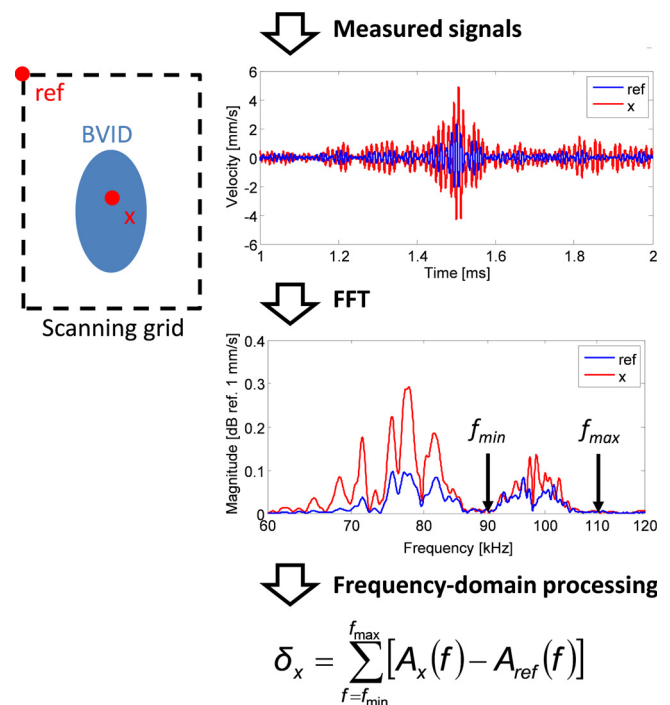


FIG. 3. Signal post-processing steps involved in the imaging of the BVID in the composite plate once the elastic waves energy has been focused sequentially at all the points of the scanning grid.



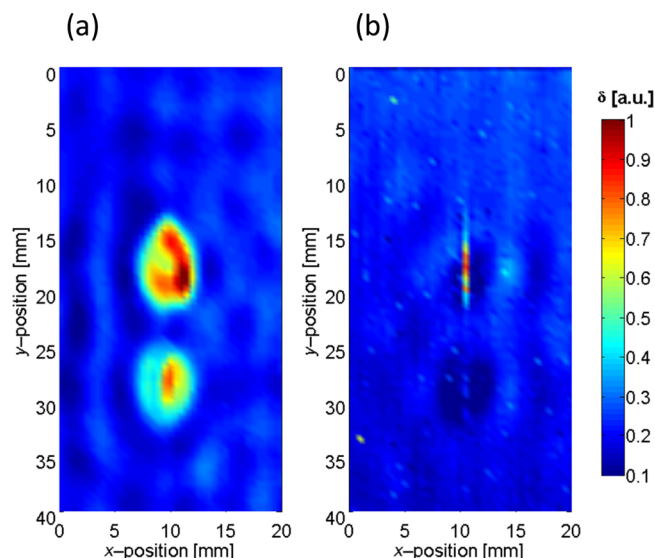


FIG. 4. Imaging of the BVID in the composite plate with the TRM and frequency-domain linear post-processing. Images were obtained by focusing the (a) out-of-plane and (b) in-plane (along the  $x$ -direction) components of the particle velocity at each point of a scanning grid on the surface of the composite plate. The delamination (or crack) can be imaged when the out-of-plane (or in-plane) component of the velocity is used in the TR process.

bounds is preferred in this case because it leads to a better imaging resolution.

Imaging of the BVID was achieved by using the TRM and the post-processing technique described earlier. Two sets of experiments were conducted with the same TRM but with a different receiver, in order to achieve either out-of-plane or in-plane focusing. Out-of-plane focusing reveals the two delaminations of the BVID, as shown in Fig. 4(a). The crack, on the other hand, is readily apparent with in-plane focusing, as shown in Fig. 4(b). The in-plane focusing direction is normal to that of the crack. If it is aligned with the crack, then the crack can no longer be identified. For the same reason, the crack cannot be imaged with out-of-plane focusing or with a C-scan at normal incidence and the delamination cannot be imaged with in-plane focusing. Therefore, the features of the BVID can be decoupled and imaged independently by focusing on different motion components of the plate. It seems that the focused motion component should be aligned with the direction of the largest gradient of elastic properties induced by the damage. For instance, a delamination creates a local change of the bending stiffness in the plate, which can be best imaged with out-of-plane focusing. Note that the features of the BVID imaged with the TRM are the same as those imaged with vibrothermography, but their size is smaller, possibly because the air-coupled TRM can only image the open regions of the damage or because vibrothermography overestimated the size due to thermal diffusion. To open and image the closed regions of the damage (near the crack tips and delamination edges), more energy should be injected into the system. It is worth mentioning that these tests were conducted in a plate of uniform thickness away from its edges. Given the linear signal processing technique that we used, it is expected that a change in the boundary conditions within the plate, due to the presence of stiffeners, would be

detected as a defect. The sensitivity to boundary conditions can be minimized and possibly removed by the use of signal processing techniques based on the nonlinear elastic response of the defect.<sup>7,8</sup> However, such study is outside the scope of this letter.

In summary, we demonstrated that an air-coupled TRM can be used to image a complex defect buried in a plate. Unlike conventional air-coupled transducers, this device can excite selectively vector components of motion into the object. This capability, inherited from the principle of TR, allows decoupling the features of the defect according to their orientation. This was demonstrated in this letter by using a laminated composite plate with a BVID fully characterized with two traditional NDT techniques.

We gratefully acknowledge the support of the U.S. Department of Energy through the LANL/LDRD Program and the Foundation for Polish Science (FNP) within the scope of the WELCOME Programme – Project No. 2010-3/2. In addition, we would like to acknowledge Professor Francesco Aymerich, at Università degli Studi di Cagliari, for providing the test sample and laboratory facilities to perform C-scan testing.

- <sup>1</sup>D. E. Chimenti, *Ultrasonic* **54**(7), 1804 (2014).
- <sup>2</sup>M. C. Remillieux, B. E. Anderson, T. J. Ulrich, P.-Y. Le Bas, M. R. Haberman, and J. Zhu, *Acoust. Today* **10**(3), 36 (2014).
- <sup>3</sup>J.-H. Song, D. E. Chimenti, and S. D. Holland, *J. Acoust. Soc. Am.* **119**(2), 1 (2006).
- <sup>4</sup>X. Dai, J. Zhu, and M. R. Haberman, *J. Acoust. Soc. Am.* **134**(6), EL513 (2013).
- <sup>5</sup>L. Azar, Y. Shi, and S.-C. Wooh, *NDT&E Int.* **33**(3), 189 (2000).
- <sup>6</sup>M. Fink and C. Prada, *Inverse Prob.* **17**(1), R1 (2001).
- <sup>7</sup>T. J. Ulrich, P. A. Johnson, and R. A. Guyer, *Phys. Rev. Lett.* **98**(10), 104301 (2007).
- <sup>8</sup>T. J. Ulrich, A. M. Sutin, T. Claytor, P. Papin, P.-Y. Le Bas, and J. A. Ten Cate, *Appl. Phys. Lett.* **93**(15), 151914 (2008).
- <sup>9</sup>P.-Y. Le Bas, T. J. Ulrich, B. E. Anderson, R. A. Guyer, and P. A. Johnson, *J. Acoust. Soc. Am.* **130**(4), EL258 (2011).
- <sup>10</sup>C. Draeger and M. Fink, *Phys. Rev. Lett.* **79**(3), 407 (1997).
- <sup>11</sup>A. M. Sutin, J. A. TenCate, and P. A. Johnson, *J. Acoust. Soc. Am.* **116**(5), 2779 (2004).
- <sup>12</sup>O. Bou Matar, Y. F. Li, and K. Van Den Abeele, *Appl. Phys. Lett.* **95**(14), 141913 (2009).
- <sup>13</sup>N. Etaix, M. Fink, and R. K. Ing, *J. Acoust. Soc. Am.* **131**(5), EL395 (2012).
- <sup>14</sup>P.-Y. Le Bas, T. J. Ulrich, B. E. Anderson, and J. J. Esplin, *J. Acoust. Soc. Am.* **134**(1), EL52 (2013).
- <sup>15</sup>N. Etaix, J. Dubois, M. Fink, and R.-K. Ing, *J. Acoust. Soc. Am.* **134**(2), 1049 (2013).
- <sup>16</sup>K. L. Reifsnider, E. G. Henneke, and W. W. Stinchcomb, “The mechanics of vibrothermography,” in *Mechanics of Nondestructive Testing*, edited by W. W. Stinchcomb (Plenum, New York, 1980), pp. 249–276.
- <sup>17</sup>L. Pieczonka and M. Szwedo, “Vibrothermography,” in *Advanced Structural Damage Detection: From Theory to Engineering Applications*, edited by T. Stepinski, T. Uhl, and W. J. Staszewski (Wiley, 2013), pp. 233–261.
- <sup>18</sup>L. Pieczonka, F. Aymerich, and W. J. Staszewski, *Procedia Eng.* **88**, 216 (2014).
- <sup>19</sup>M. C. Remillieux, B. E. Anderson, P.-Y. Le Bas, and T. J. Ulrich, *Ultrasonics* **54**(5), 1409 (2014).
- <sup>20</sup>B. E. Anderson, M. C. Remillieux, P.-Y. Le Bas, T. J. Ulrich, and L. Pieczonka, *Ultrasonics* **63**, 141 (2015).
- <sup>21</sup>M. A. Mironov, *Sov. Phys. Acoust.* **34**(3), 318 (1988).
- <sup>22</sup>V. V. Krylov, *Moscow Univ. Phys. Bull.* **45**(6), 65 (1990).
- <sup>23</sup>T. J. Ulrich, K. Van Den Abeele, P.-Y. Le Bas, M. Griffa, B. E. Anderson, and R. A. Guyer, *J. Appl. Phys.* **106**, 113504 (2009).